White paper

Striatal analysis in *syngo*.via MI Neurology

Rachid Fahmi, PhD
Guenther Platsch, MD

siemens-healthineers.com

SIEMENS Healthineers

Table of contents

Introduction

Parkinsonian syndromes are a group of movement disorders that share a common set of symptoms characterized by bradykinesia, tremor at rest, and rigidity. Most frequently, these syndromes are due to the degeneration of the dopaminergic neurotransmitter system (DNS). Examples of such neurodegenerative syndromes include idiopathic Parkinson's disease (PD), multiple system atrophy, progressive supranuclear palsy, corticobasal degeneration, and dementia with Lewy bodies. Other parkinsonian etiologies don't involve dopaminergic degeneration and can either be drug-induced, vascular, or of psychogenic nature. Patients suffering from presynaptic neurodegeneration may benefit from dopaminergic medication.

Parkinson's disease accounts for 75% of all cases of parkinsonism[1] and is considered to be the second most common neurodegenerative disorder after Alzheimer's disease, with 10 million people affected worldwide, and 60,000 newly diagnosed patients in the US each year. Clinical diagnosis of PD can be straightforward and often does not require additional tests.[2] However, diagnosis can be inconclusive for cases with atypical, unclear, and concurrent conditions which might have adverse prognosis implications in the disease management.[2, 3] For such cases, functional imaging of the DNS may improve diagnosis accuracy.

Dysfunction of the presynaptic dopaminergic system is the primary cause of the dominant motor features in PD.[4] This system can be analyzed at the striatal level where dopaminergic neurons end and interact with the postsynaptic neurons using dopamine as the neurotransmitter.[2]

Dopamine is a neurotransmitter produced by the dopaminergic neurons, with a central role in the regulation and control of movement. Dopaminergic neurons project from the substantia nigra pars compacta to the striatum (caudate and putamen) where dopamine is synthesized via dopa decarboxylase function and stored in vesicles. When the appropriate signal is received, dopamine is released to the synaptic cleft (SC) and interacts with postsynaptic dopamine receptors. Dopamine transporters (DAT) take back extracellular dopamine from the SC into the presynaptic nerve terminals for either storage or degradation (see Figure 1). This DAT function helps regulate dopamine levels and enables response to other signals.

Presynaptic parkinsonism, which includes PD, is predominately characterized by nigrostriatal degeneration resulting in loss of dopaminergic neurons which in turn results in loss of DATs in the striatum. Conversely, DAT density is generally normal in non-degenerative parkinsonism (eg, essential tremor).

Different molecular imaging tracers have been developed to assess the integrity of the nigrostriatal system in patients with suspected neurodegenerative parkinsonism and for the differentiation between Alzheimer's disease and dementia with Lewy bodies.[5-7] For example, the ligand N-ω-fluoropropyl-2β-carbomethoxy-3β-(4-I-123-iodophenyl) nortropane (^{123}I-FP-CIT[a] or ^{123}I-ioflupane; brand name: DaTscan™, GE Healthcare) is a single photon emission (SPECT) cocaine analogue with high binding affinity to DATs, whereas 6-[^{18}F]fluoro-L-DOPA (^{18}F-DOPA[a] or simply FDOPA[a]) is a positron emission tomography (PET) tracer that provides an indirect measure of the dopaminergic neurons' density through the evaluation of the enzymatic dopa-decarboxylase (DDC) activity within these neurons.[8] With progressive degeneration of the nigrostriatal system, DDC activity will be reduced, and this reduction is reflected on FDOPA[a] images as low uptake in the striatum.

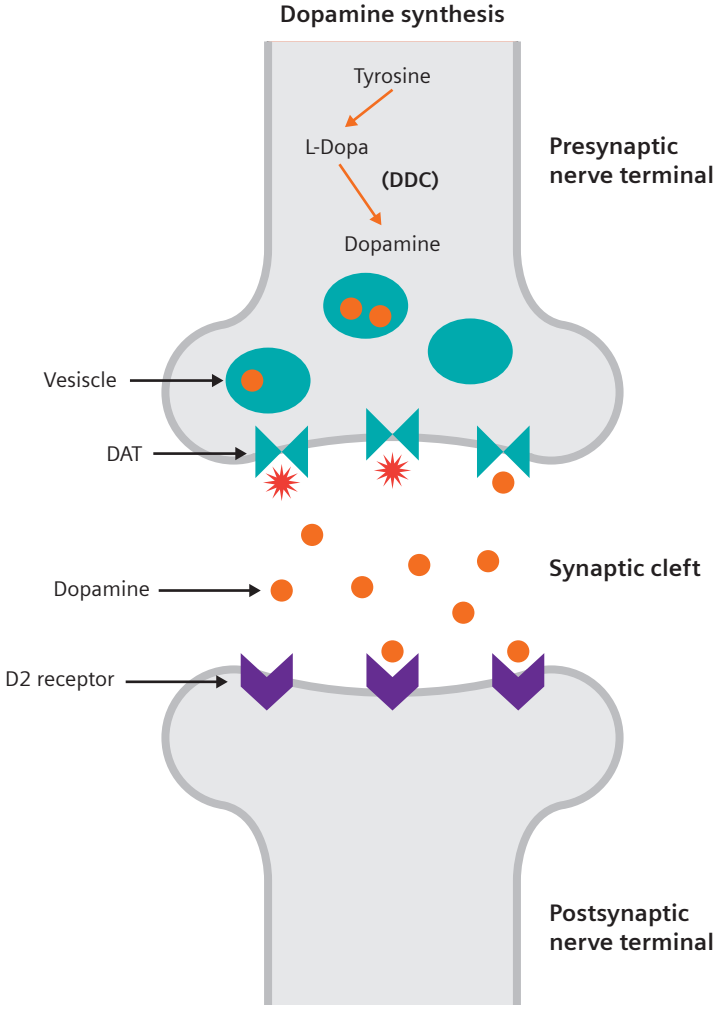

Figure 1. Schematic of the striatal dopaminergic pathway. Dopamine is synthesized and stored in vesicles. On excitation, dopamine is released to the synaptic cleft (SC) and interacts with postsynaptic dopamine receptors. Dopamine transporters (DAT) move extracellular dopamine from the SC back into the presynaptic neuron. Stars indicate where ^{123}I-FP-CIT[a] binds. DDC: dopa decarboxylase activity.

Practice guidelines for DAT imaging with ^{123}I-FP-CIT[a] have been developed by the European Association of Nuclear Medicine (EANM) and by the Society of Nuclear Medicine and Molecular Imaging (SNMMI).[2, 9]

Other ligand tracers used to evaluate the key functions of dopaminergic neurotransmission include ^{123}I-β-CIT[a] and ^{99m}Tc-TRODAT-1[a] for SPECT and ^{18}F-FP-CIT[a] for PET.

^{123}I-FP-CIT[a] and FDOPA imaging in Parkinson's disease

For patients with nigrostriatal degeneration, both ^{123}I-FP-CIT[a] and FDOPA[a] images show reduction in uptake in the basal ganglia, whereas images of healthy subjects show an intense and symmetrical tracer uptake in both striata as shown in Figure 2. According to practice guidelines, the interpretation of such images is based on visual evaluation of the reconstructed images which raised questions as to the reproducibility of the technique,[10] in particular for equivocal cases. Furthermore, visual interpretation can be especially challenging in a follow-up situation to differentiate relevant changes from irrelevant ones.

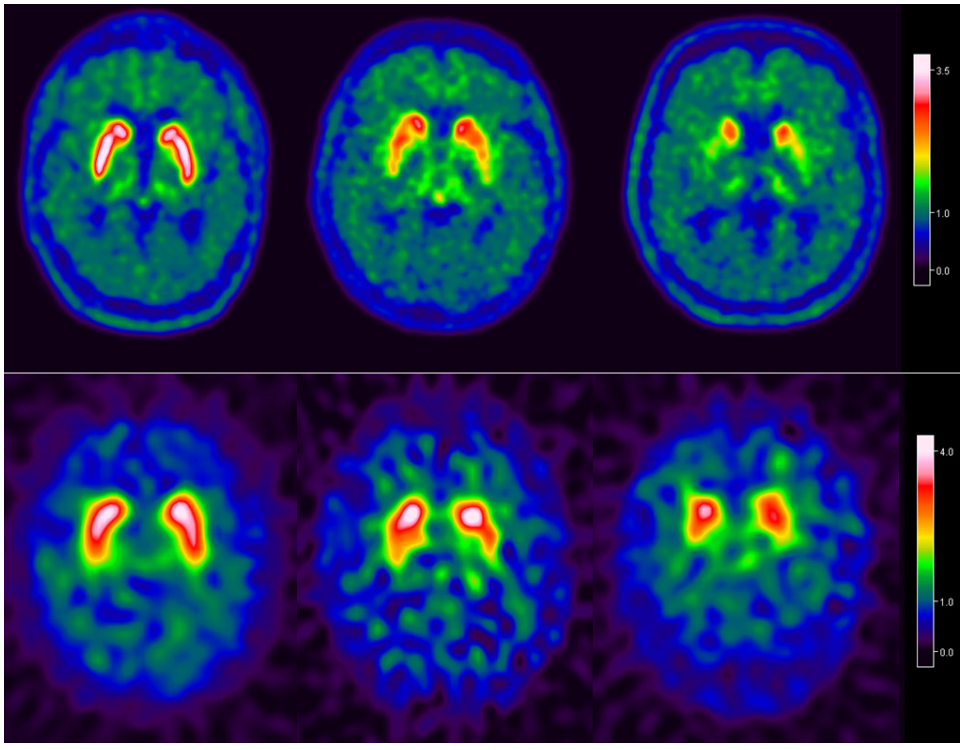

Figure 2. Axial FDOPA[a] (upper row) and ^{123}I-FP-CIT[a] (bottom row) slab views (see "Visual Interpretation" section) through the striatum. From left to right, the images show a normal symmetrical uptake, an asymmetric uptake with a clear reduction in left putamen, and a more severe case with substantial uptake reduction in both putamina.

Data courtesy of Centre Antoine Lacassagne, Nice, France and Hospices Civils de Lyon, Lyon, France.

Various studies as well as the EANM[9, 11-15] recommend semi-quantitative analysis of DAT images for an objective evaluation of striatal DAT availability. Various semi-quantitative analysis techniques using region-of-interest (ROI)-based approaches[11-15] or more sophisticated automatic classification procedures[16-18] have been developed. These methods can help to align visual interpretation of striatal images. However, the procedure guidelines of the SNMMI acknowledges that there is no evidence-based answer as to whether semi-quantitative analysis of ^{123}I-FP-CIT[a] images helps an inexperienced reader in routine clinical settings to perform a better evaluation compared to visual reading alone. Therefore, SNMMI advises that visual interpretation is generally sufficient in clinical patient care.[2] This discrepancy between current practice guidelines reflects the fact that both qualitative interpretation and semi-quantitative analysis have pitfalls.[19]

Striatal Analysis within *syngo*®.via MI Neurology is a software solution that enables the user to perform accurate visual reads of both FDOPA[a] and ^{123}I-FP-CIT[a] images (and other dopaminergic neurotransmission ligands, as well as for dopamine 2 receptor (D2) ligands such as ^{123}I-IBZM (iodobenzamide) and ^{11}C-raclopride). It uses a semi-quantitative slab view with a standardized orientation and intensity scaling.[19-20] It also performs a fully automated volume of interest (VOI) analysis and quantify uptake ratios and asymmetry values in different striatal regions. Furthermore, the workflow also allows the user to create custom-built databases of normal reference binding values and use them to assess new scans.

The purpose of this white paper is to describe the tools provided by Striatal Analysis, as available in *syngo*.via MI Neurology, for use with a typical analysis and to provide technical details about the processing applied to data during the analysis.

Automated semi-quantitative analyses

Striatal Analysis is based on a set of processing steps that automatically position the input image in a standardized stereotactic space and display a two-dimensional (2D) view of the striatum as an average of a 12 mm thick (6 slices of 2 mm each) transversal slab of intensity-scaled voxel values through left and right striata using a standard color table. Distribution volume ratios and asymmetry values are automatically calculated within predefined striatal volumes of interest in the standardized stereotactic space and displayed graphically (when compared to normal references) and in a tabular fashion.

Creation of a standardized template

The first step performed by Striatal Analysis software after loading new exam data is the automatic stereotactic normalization of the patient's functional image to an appropriate PET or SPECT template in the anatomical space of the Montreal Neurological Institute (MNI). The SPECT and PET MNI templates were created through an iterative process using respective scans from patients with a wide range of striatal uptake (FDOPA[a]: 30 subjects, 15 male and 15 female, age: 72.0±11.0 years; ^{123}I-FP-CIT[a]: 20 scans, 13 F, 7 M, age: 67.3±11.5 years).

For each tracer, the iterative process (eg, see Buchert et al[19] for ^{123}I-FP-CIT[a]) involves automatic affine registration of a set of images to an intermediate template in the MNI space. Registration results are visually assessed and if considered to be acceptable, the registered images are intensity normalized and averaged to create an updated version of the intermediate template. The process is iterated until the number of successful registration operations ceases to increase. Intensity normalization is performed voxel-wise by dividing each voxel value by the mean uptake in an occipital lobe region predefined in the MNI space (eg, see green outlined region in Figure 5). The final template is symmetrized by averaging the voxel values with the template mirrored around the midline of the brain. This iterative template creation process was initiated by the creation of a functional template in the MNI space using computed tomography (CT)-based affine registration of hybrid (SPECT/CT or PET/CT) image pairs from two patients. Figure 3(a-b) show axial, coronal, and sagittal views of the created FDOPA[a] and ^{123}I-FP-CIT[a] templates in the MNI standard space.

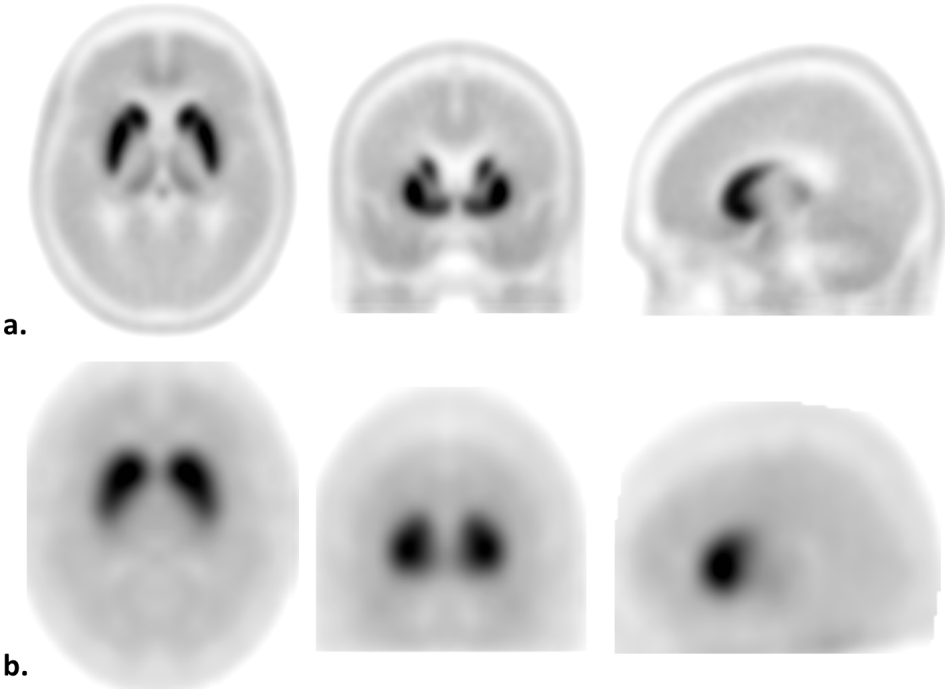

Figure 3. Axial, coronal and sagittal views of (a) FDOPA[a] and (b) ^{123}I-FP-CIT[a] templates in the Montreal Neurological Institute (MNI) space.

Data courtesy of Siemens Medical Solutions USA, Inc.

Creation of striatal volumes of interest

Quantification of both FDOPA[a] and ^{123}I-FP-CIT[a] images is based on an automated three-dimensional (3D) VOI analysis in the standard MNI space. For ^{123}I-FP-CIT[a], the striatal VOIs are created by first using a threshold-based segmentation of the left and right striata (caudate and putamen) from the ^{123}I-FP-CIT[a] template image. Then, the separation of caudate and putamen is performed using a cutting plane that is positioned parallel to the plane separating caudate and putamen in a magnetic resonance (MR) template in the MNI space. For FDOPA[a], the striatal VOIs are created as smoothed and morphologically transformed versions of the left and right striatal regions defined in the automated anatomical labeling (AAL) atlas.[21] For both modalities, the VOIs are slightly enlarged to ensure their complete enclosure of anatomical structures[22] independent of some residual anatomical interpatient variability after spatial transformation of images to the standard MNI space. The final volumes of caudate and putamen, for both modalities, are: caudate (11 ml and 7.3 ml) and putamen (9 ml and 12 ml) for ^{123}I-FP-CIT[a] and FDOPA[a], respectively.[22]

As the posterior putamen is the most and earliest-affected structure of the striatum,[23] the left and right putaminal regions are split into two parts: anterior and posterior. This splitting is performed so that the volume of the anterior region is about 10% larger than that of the posterior region. Figure 4 shows the generated striatal FDOPA[a] and ^{123}I-FP-CIT[a] striatal VOIs.

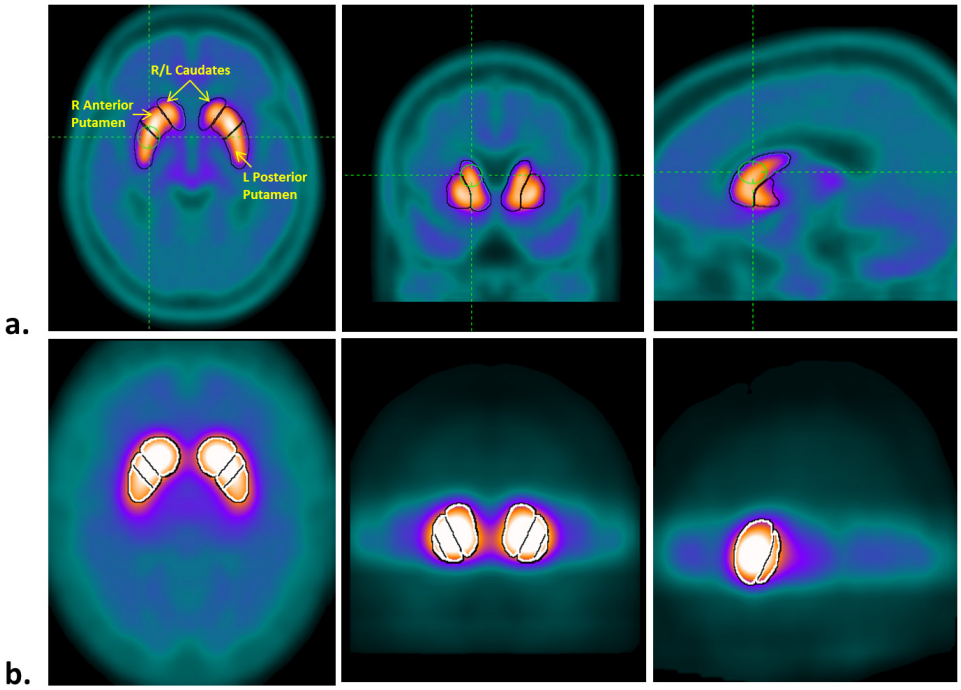

Figure 4. Axial, coronal and sagittal views showing predefined striatal regions of interest overlaid on the (a) FDOPA[a] and (b) ^{123}I-FP-CIT[a] standard templates. R: right, L: left.

Data courtesy of Siemens Medical Solutions USA, Inc.

VOI-based semi-quantitative analysis

The fully automated VOI analysis completed with Striatal Analysis in *syngo*.via MI Neurology is based on the full 3D SPECT image being analyzed, instead of just the slab view. Standard left and right striatal VOIs (caudate, putamen, anterior and posterior putamina, and whole striatum) predefined in the MNI space, as described above, are used to compute regional parameters (binding ratios and asymmetry values).

The first step in Striatal Analysis is to spatially normalize the patient's input functional image to the corresponding template in the MNI space (using a 12-parameter affine registration). The registration quality can be assessed visually and if required, the user can make manual adjustments using a 3D affine transform (translation, rotation, scaling, and shear). In addition, if a patient's brain CT scan is available, it can be used to guide the registration of the functional scan to the standard template in case the automatic functional-based registration (default setting) is suboptimal.

In a second step, the predefined striatal VOIs (in the MNI space) are automatically placed on the spatially normalized patient's image as shown in Figure 5. The user can also make manual adjustments (translations and rotations) of the VOIs' positions if necessary.

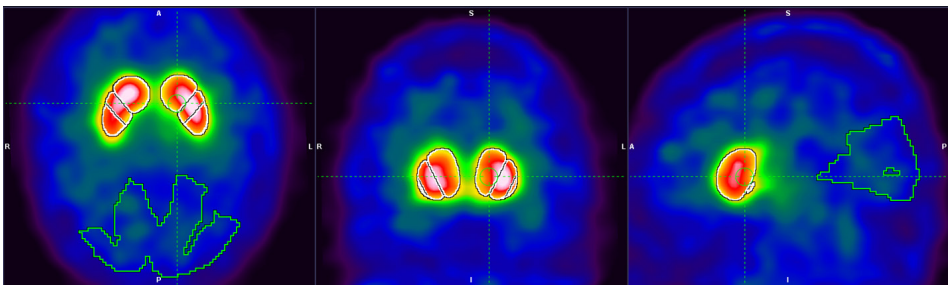

Figure 5. Automatic placement of striatal (white contours) and background (occipital lobe: green contour) VOIs on the spatially normalized patient's ^{123}I-FP-CIT[a] image.

Data courtesy of Hospices Civils de Lyon, Lyon, France.

Distribution volume ratios (DVR) are then automatically computed on each VOI as the mean of the 75% brightest voxels within the target VOI divided by the mean uptake in the occipital lobe VOI (computed using all voxels). The occipital lobe VOI is also automatically placed on the spatially normalized image (green contour in Figure 5) and can also be edited and its position manually adjusted if needed.

The left and right putamen-to-caudate ratios as well as asymmetry values between both hemispheres are computed in addition to DVR values. The asymmetry value between the left and right side of a given VOI is calculated as:

$$\text{asym (\%)} = 100 \times \text{abs}(DVR_{left} - DVR_{right}) / [(DVR_{left} + DVR_{right})/2],$$

where DVR_{left} and DVR_{right} correspond to the DVR values computed on left and right sides of the target VOI, respectively.

Visual interpretation

The interpretation of both ^{123}I-FP-CIT[a] and FDOPA[a] data is based in part on visual evaluation of the reconstructed images. As mentioned earlier, procedure guidelines of both EANM and SNMMI for ^{123}I-FP-CIT[a] SPECT recommend visual evaluation of the tomographic images. However, unlike SNMMI which considers that visual interpretation alone is generally sufficient in clinical patient care, EANM considers semi-quantitative analysis mandatory for an objective evaluation of DAT availability. This discrepancy in practice guidelines is partially due to the way visual reads are routinely conducted, typically using an inappropriate color table to display uptake images by scaling the maximum voxel intensity to the brightest color in each image. The maximum voxel intensity in ^{123}I-FP-CIT[a] and FDOPA[a] images often occurs in the striatum for both normal patients and patients with degeneration of the dopaminergic neurotransmitter system. In a recent publication,[19] authors proposed the use of a semi-quantitative slab view display optimized for visual evaluation of ^{123}I-FP-CIT[a] images and argued that such a display might resolve the discrepancy between practice guidelines. This slab view display has been adopted for ^{123}I-FP-CIT[a] and FDOPA[a] data in Striatal Analysis.

Using Striatal Analysis, the slab view display is generated as follows. First, the spatially normalized patient's uptake image is scaled voxel by voxel to the mean uptake in a standard whole-brain VOI predefined in the MNI space with a cavity encompassing the left and right striata. The resulting DVR image is then used to generate a 12-mm-thick transversal slice (slab) centered (in axial direction) at the striatum in the MNI space. The advantage of displaying the DVR image over the input functional uptake image is that its voxel intensities carry a quantitative value. The DVR image can be displayed with a predefined color table and an optimized upper threshold.[19] It is recommended that this threshold be determined independently for each combination of acquisitions and reconstruction protocols. The use of standardized DVR slab views for visual interpretation of ^{123}I-FP-CIT[a] images was proven to provide excellent inter- and intra-observer agreement and to highly concur with semi-quantitative analysis.[19] An example of a slab view generated by Striatal Analysis is shown in Figure 6 with a 'spectrum' color table and an upper DVR threshold equal to 4.0.

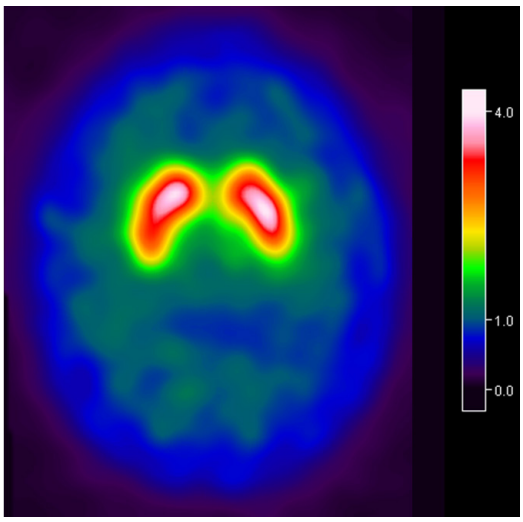

Figure 6. Standardized slab view display using a DVR threshold of 4.0 for a patient with symmetrical striatal uptake.

Data courtesy of Hospices Civils de Lyon, Lyon, France.

Construction of a Striatal Database

Computation of DVRs, putamen-to-caudate ratios, and asymmetry values on different striatal regions with respect to a reference VOI was introduced in an earlier version of Striatal Analysis in *syngo*.via MI Neurology. However, quantitative measures have little clinical value without reference ranges, especially for equivocal cases and for early disease stages, when diagnostic decisions cannot be drawn from quantitative results as the scans cannot be interpreted visually as abnormal.[25] These complex cases could be better interpreted if normative data, eg, derived from a cohort of normal controls, are available. Hence, we have developed and introduced a framework that allows users to create their own normal ranges of different parameters. For age-dependent dopaminergic PET and SPECT tracers, such as ^{123}I-FP-CIT[a], the tracer's age dependency is accounted for in the database construction process.

A key aspect in building a database is to ensure that the same set of processing operations is applied to each dataset selected to be included. In addition, the selected 'normal' scans should all be acquired, reconstructed, and corrected using the same protocols. When comparing a new subject to an available database, patient protocol should adhere to the above settings to avoid systematic differences caused by acquisition or reconstruction.

The user can determine the criteria of normalcy of a scan as well as the age distribution of the normal population to be included in a custom database. Subjects can be categorized as normal if they have functional and anatomical scans free of abnormalities (eg, negative SPECT scan and normal CT) and no confirmed neurodegenerative parkinsonism, both at baseline and after a well-defined follow-up period (≥3 years). Scans selected for inclusion in a normal database must all be processed following the same steps of the Striatal Analysis pipeline to calculate their respective DVR and asymmetry values. These values are used to generate reference statistics (means, standard

deviations, z-scores, prediction intervals, etc.). For each striatal region, the corresponding right and left reference DVR values are assumed to not significantly differ from one another (ie, low or no asymmetries) and are averaged to estimate a single regional reference value. However, when comparing a test subject to an available database, for each VOI, the subject's right and left values are separately compared to their corresponding reference value.

In the case of ^{123}I-FP-CIT[a], the age of every patient is recorded, and an age-correction is applied through linear regression to model the normal decrease of uptake with age.[28] This is not the case for FDOPA[a] as there is no strong evidence supporting ageing effect on FDOPA[a] uptake.[26, 27] In addition, findings about the effect of gender on DAT availability have not been consistent in the published literature.[24, 28]

Once a user-defined database is constructed, the user can edit and view it as well as add new subjects to it or delete existing ones. However, databases provided with the system cannot be edited or modified.

Comparison to a normal database

The first step when commencing Striatal Analysis of a new subject study is to select an appropriate database. Such a database could be either custom-built or provided within *syngo*.via, but in general the following items should be considered when selecting a database for comparison:

- What modality and tracer were used to image the new subject? In case of a SPECT scan, what collimators were used during acquisition?
- What reconstruction algorithm (eg, Flash3D or Filtered Back Projection (FBP)) was used to reconstruct the subject's dataset? What scatter correction and post-reconstruction filters were used?
- What type of attenuation correction was used during reconstruction (eg, Chang or CT-based)?
- Was the same background region used to analyze and quantify the subject's data as the one used to generate the reference values?

If any of the above items are not matched between the selected database and the new subject, it is possible that the comparison findings could be artifacts unrelated to the subject's disease status. Ideally, a database would be selected that exactly matched the subject image in terms of the above parameters; however, in practice there is some tolerance in the parameters, especially when smoothing is used. Importantly, differences between the database parameters and subject image should be considered during analysis.

A new subject's ^{123}I-FP-CIT[a] image can be compared to an available database only if the subject's age is within ten years from the database age range. New subjects whose age is outside of this range, or those whose age information is missing can still be uploaded using Striatal Analysis, processed and their DVR and asymmetry values calculated and displayed but no comparison results would be generated. This restriction does not apply to FDOPA[a] as no age correction is necessary during quantification or comparison to normative values.

System Striatal Databases

One FDOPA[a] and two ^{123}I-FP-CIT[a] databases are available in *syngo*.via for use within Striatal Analysis. Following are the detailed descriptions of these databases.

Individual database details: FDOPA-PET

The system FDOPA[a] database was built using 53 data sets acquired on a Biograph mCT scanner at Centre Antoine Lacassagne, Nice, France. All subjects were orally premedicated with 100 mg of carbidopa[29] one hour prior to the intravenous injection of 2.5-6 mCi of ^{18}F-DOPA. Scanning followed 1.5-2 hours after tracer injection. PET data images were reconstructed using OSEM3D with 5 iterations and 24 subsets, and with scatter correction using a model-based method and CT-based attenuation correction. More details about the created database are summarized in Table 1.

The included subjects in our database were not healthy volunteers, but patients who were referred to the imaging site with a neurological condition but had a negative FDOPA[a] scan and no evidence of neurodegenerative parkinsonism both at baseline and during a follow-up exam ≥18 months.

Table 1. Characteristics of FDOPA[a] database.

Name	**FDOPA1A**
Acquisition	Biograph mCT
Reconstruction	OSEM3D with SC and CT-AC, 5 iterations, 24 subsets, 4 mm Gauss filter
Registration	PET or CT-based affine
Reference region	Occipital lobe (100% brightest voxels)
Number of subjects	53
Age range	42-90 (73.4 ± 9.2)
Gender	Mixed (33 female, 20 male)
Data source	Centre Antoine Lacassagne, Nice, France

References values

Regional reference DVR and asymmetry values as well as left and right putamen-to-caudate ratios (P/C) were computed as described above. No age or gender effects were observed on the quantified parameters. Figure 7 summarizes the generated reference values.

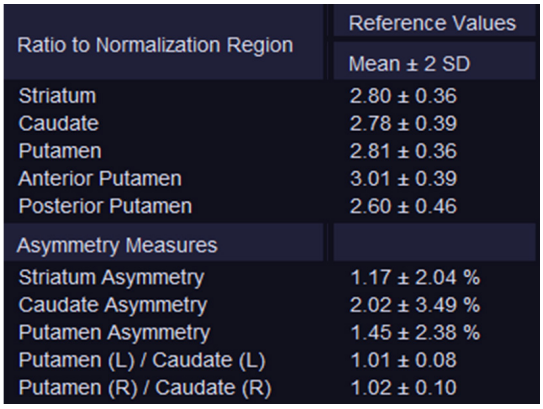

Ratio to Normalization Region	Reference Values
	Mean ± 2 SD
Striatum	2.80 ± 0.36
Caudate	2.78 ± 0.39
Putamen	2.81 ± 0.36
Anterior Putamen	3.01 ± 0.39
Posterior Putamen	2.60 ± 0.46
Asymmetry Measures	
Striatum Asymmetry	1.17 ± 2.04 %
Caudate Asymmetry	2.02 ± 3.49 %
Putamen Asymmetry	1.45 ± 2.38 %
Putamen (L) / Caudate (L)	1.01 ± 0.08
Putamen (R) / Caudate (R)	1.02 ± 0.10

Figure 7. Generated reference values (mean ± 2×standard deviations) for the FDOPA[a] database.

Individual database details: ^{123}I-FP-CIT[a] SPECT

From a pool of 1,884 patients scanned on a Symbia™ T2 with low-energy, high-resolution collimators (LEHR) between January 2008 and December 2015, we received datasets corresponding to 256 consented subjects (raw SPECT data and attenuation correction CT scans) from the nuclear medicine department of the Hospices Civils de Lyon, France. All scans were acquired three hours post intravenous injection of ~185 MBq of ^{123}I-FP-CIT[a] which occurred one hour following thyroid blockade (perchlorate) when needed.

These subjects were not healthy volunteers, but are patients who were referred to the imaging center with a neurological condition (eg, essential tremor or drug-induced parkinsonism) but had a negative ^{123}I-FP-CIT[a] exam and no confirmed neurodegenerative parkinsonism at baseline nor at a follow-up period between 3 and 10 years (4.8 ± 1.3 years). Table 2 summarizes final clinical diagnoses for all included subjects. On-site (Lyon, France) analyses of all ^{123}I-FP-CIT[a] exams were performed based on visual interpretation by two expert readers and on semi-quantitative analysis using an in-house software. Note that this analysis program is independent of the software application implemented in *syngo*.via, which was used to generate our ^{123}I-FP-CIT[a] reference values.

Table 2. Final diagnoses of subjects included in the generated ^{123}I-FP-CIT[a] databases.

Diagnostic	Ratio (%)	n
Essential tremor	27.0	64
Drug induced parkinsonism	22.8	54
Dementia without dopaminergic degeneration (AD or frontotemporal dementia)	10.5	25
Miscellaneous or mixed (rheumatologic disorders, myopathy, primary lateral sclerosis, epilepsy, ...)	10.1	24
Attentional deficit hyperactivity disorder	8.5	20
Psychiatric disorders, psychogenic parkinsonism or movement disorders	6.3	15
Vascular parkinsonism without dopaminergic degeneration	6.1	14
Normal pressure hydrocephalus	2.5	6
Dystonia	1.3	3
Restless legs syndrome	1.3	3
Amyotrophic lateral sclerosis	0.8	2
Epilepsy	0.8	2
Orthostatic tremor	0.8	2
Genetic parkinsonism	0.8	2
Cerebellar ataxia	0.5	1
Total	100%	237

Prior to building the databases, further quality checks of the data were performed by a trained physician looking for any severe patient motion in the SPECT projection data and/or any reconstruction or imaging artifacts, as well as any anatomical abnormalities (eg, major hydrocephalus or atrophies) in the CT images. The final diagnoses as well as the clinical reads of the SPECT images of all subjects were assessed when selecting which subjects to include in the databases. Some of the excluded subjects had severe head motion, major hydrocephalus, and/or were suspected of having an abnormal reduced uptake based on a visual assessment of the subject's slab view.

Finally, data corresponding to a total of 237 subjects (120 male, 117 female, age: 62.2±15.7 years, range: 16-88 years were used to build two normal databases corresponding to two different image reconstruction methods: a) Flash3D reconstruction with CT attenuation correction, triple energy window (TEW) scatter correction, and ten iterations and eight subsets; and b) FBP reconstruction with Chang attenuation correction, and Butterworth filter of order five and a cut-off frequency of 0.45 cycles/pixel. Characteristics of these databases are summarized in Table 3. A detailed description of the created FP-CIT databases, including the two-step patient selection process, and comparison against a database from healthy volunteers can be found in Rahmi et al.[30]

Table 3. Characteristics of the reconstructed system ^{123}I-FP-CIT[a] databases.

Name	FPCIT1A	FPCIT2A
Acquisition	Symbia™ SPECT•CT	
Reconstruction	Flash3D with CT-AC, 10 iterations, 8 subsets, 8 mm Gauss filter, matrix size 128 x 128, zoom factor 1.23 x 1.23	FBP with Chang AC (μ=0.11cm-1), Butterworth filter (order = 5, cut-off frequency = 0.45 cycles/pixel), matrix size 128 x 128, zoom factor 1.23 x 1.23
Number of projections	120 over 360°	
Rotational radius	13 -15 cm	
Registration	SPECT or CT affine	SPECT affine
Collimator	LEHR	
Scatter correction	Yes (TEW)	No
Reference region	Occipital lobe (all voxels)	
Number of subjects	237	
Age range	16-88 (62.2 ± 15.7)	
Gender	Mixed (117 female, 120 male)	
Data source	Hospices Civils de Lyon, Lyon, France	

Using *syngo*.via, the database reconstruction process follows these steps, as described above: registration of each reconstructed ^{123}I-FP-CIT[a] image to MNI space and (automatic) positioning of striatal and reference VOIs, followed by computation of regional ratios and asymmetry values using the occipital lobe as the normalization region. Other normalization regions could be used, but one has to ensure that the same normalization region is used for all data sets included in the database. To ensure accurate positioning of the striatal and reference VOIs on spatially normalized ^{123}I-FP-CIT[a] images, manual adjustments of the automatically positioned VOIs in three planes were performed whenever needed. Automatic spatial normalization of ^{123}I-FP-CIT[a] images to MNI space is sensitive to striatal uptake and to background noise characteristics, and can potentially fail in some challenging cases. This could render the adjustment of VOIs' positions difficult, even manually. In such cases, the CT-based affine registration was used to spatially normalize the SPECT image. In general, if the automatic SPECT-based registration to MNI space is suboptimal, the user can either perform a manual affine adjustment and re-launch the SPECT-based registration or use the CT-based registration if a patient's CT image is available.

Age and gender effects on DAT availability

The rate of reduction in distribution volume ratio (DVR) per decade over all subjects included in the database was between 3.15% and 4.10% depending on the reconstruction method and on the striatal region where measurements were made. This value is consistent with what has been reported in previous studies on healthy controls (between 3.6% and 7.5% per decade.[24-25, 28, 31] Note that we report DVR values whereas most of the referenced works report specific binding ratios or SBR instead, where SBR = DVR - 1). The calculated percentage declines per decade of DVR values are summarized in Table 4. Several factors, such as image reconstruction and correction as well as how quantification is performed, can contribute to the variability in the estimated percentage decline of DAT per decade seen between different published studies.

Table 4. Age-related decline in DAT availability (% per decade).

Database	Caudate	Putamen	Anterior Putamen	Posterior Putamen	Striatum
Flash3D	3.15	3.78	3.50	4.10	3.35
FBP	3.45	3.58	3.49	3.97	3.50

In agreement with multiple previous studies,[24, 32] it was noted that women have higher DVR values than men in all striatal regions regardless of the reconstruction method. Figures 8 and 9 represent the striatum DVR values for men and women in our databases (Flash3D and FBP) as a function of age. This difference tends to decline with age. As detailed in Table 5, the difference in striatal DVRs between men and women were only statistically significant (Student t-test: $p<0.05$) for the Flash3D database. The lack of such statistical significance for the FBP database may either be due to the fact that there is no correlation between gender and DAT availability or that such gender difference exists but was not statistically significant due to inaccuracies in the Chang attenuation correction method which uses a simpler approximation to individual head geometry and assumes a uniform attenuation inside the head. This may have led to more statistical noise and then to higher p values compared to using CT-based attenuation correction for the Flash3D database.

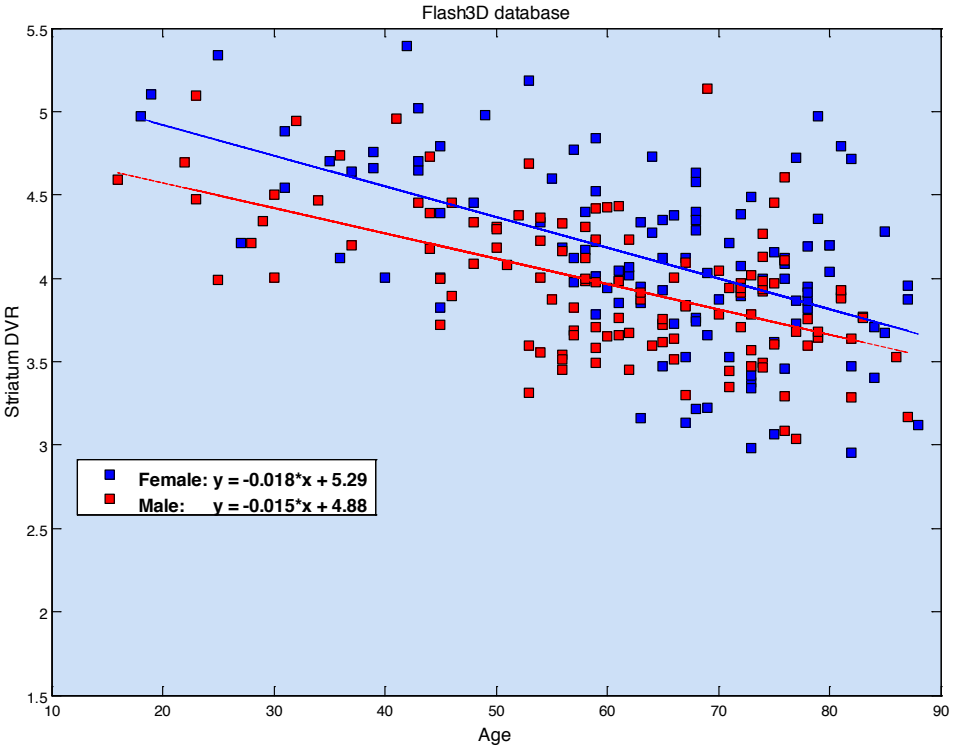

Figure 8. Effect of age and gender on DVR values computed as the average of left and right values within the striatum and plotted as a function of age. Also shown are regression lines with slope and intercept for the Flash3D database (female: blue, male: red).

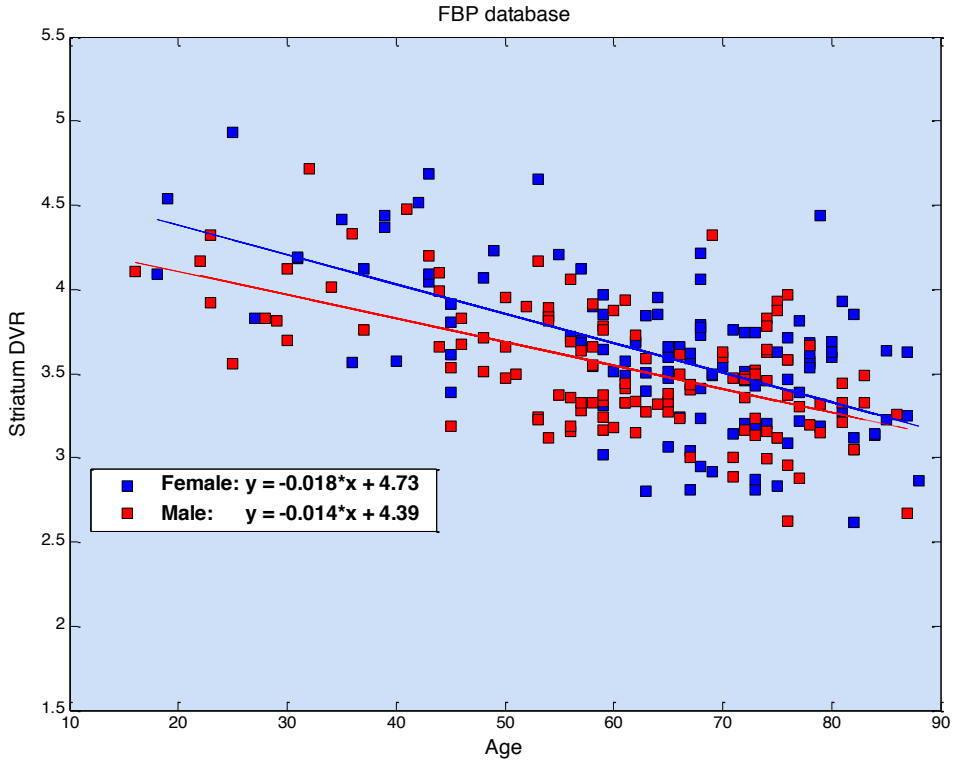

Figure 9. Effect of age and gender on DVR values computed as the average of left and right values within the striatum and plotted as a function of age. Also shown are regression lines with slope and intercept for the FBP database (female: blue, male: red).

While, based on the available datasets, the gender effect on the quantification of ^{123}I-FP-CIT[a] uptake could not be clearly shown nor excluded, identical reference values were established for both men and women. Other studies have also failed to show significant differences of DAT availability in relation to gender.[33]

Some hypotheses have been put forward to explain the higher DAT availability in women's brains compared to men's. The most likely hypothesis relates this difference in DAT availability to the difference in striatal volumes between genders.[24, 32]

Table 5. Average of left and right DVR values for Flash3D and FBP databases, for men, women, and for combined genders. Values are mean±SD. F-values and corresponding p-values are presented for the effects of age and gender on DVR.

		Flash3D			FBP		
		Striatum	Caudate	Putamen	Striatum	Caudate	Putamen
Men (n=120)		3.96±0.42	4.03±0.43	3.87±0.44	3.53±0.38	3.60±0.39	3.43±0.38
Women (n=117)		4.11±0.52	4.18±0.52	4.00±0.54	3.61±0.45	3.68±0.45	3.52±0.45
All (n=237)		4.03±0.48	4.10±0.48	3.93±0.50	3.57±0.41	3.64±0.42	3.48±0.42
F-Value	**Age**	55.19 (p<0.001)	34.66 (p<0.001)	53.85 (p<0.001)	65.57 (p<0.001)	60.88 (p<0.001)	67.02 (p<0.001)
	Gender	5.63 (p=0.018)	6.89 (p=0.009)	5.35 (p=0.022)	2.20 (p=0.14)	1.99 (p=0.16)	2.45 (p=0.12)

Age-correction using linear regression

In order to correct for the effect normal aging has on DAT availability, linear regression was performed to model the relationship between reference DVR values and patients' age. This allows for the correction of age-effects and ensures that DVR values of new subjects are compared to age-matched references. The decrease in uptake with age led to a negative linear relationship between every DVR value and age.

For each regional DVR, the standard error (SE) of the estimated regression model was used to derive the model's ±95% prediction interval. This interval is an estimate of a range where DVR values of a subject with normal striatal uptake (calculated in a similar way as the generated reference values) have a probability of 95% they will fall within predicted ranges. Example of a prediction interval is defined by the green and magenta lines in Figure 10. The lower bound (magenta line in Figure 10) is often used as a

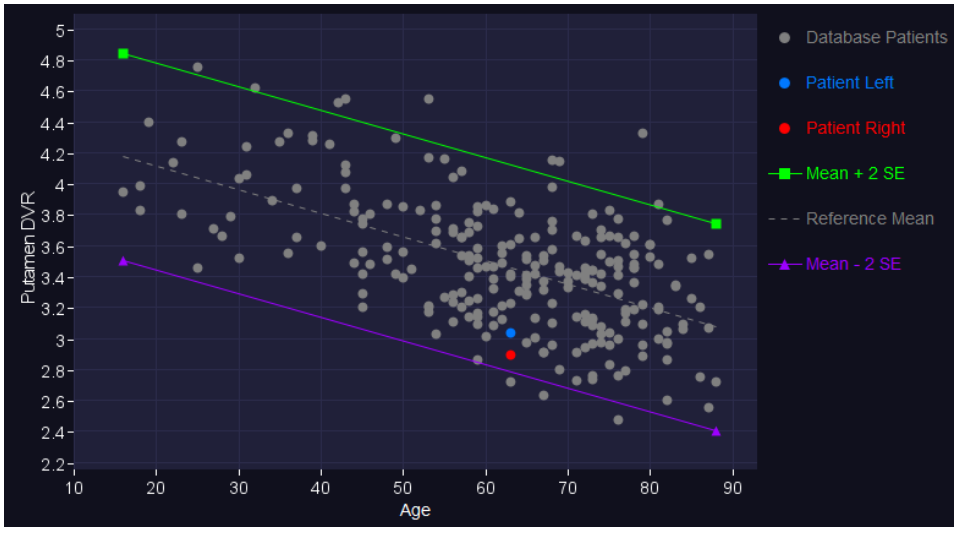

Figure 10. Scatter plot of reference DVR values computed on the putamen using FBP database. Linear regression performed to fit a line to the reference DVR values as a function of age (dashed gray line). The green and magenta lines define the ±95% prediction interval (±2×standard errors of the regression model). Red and blue dots correspond to DVR values measured within right and left putamina of a 63-year-old male. Patient's measured values are within normal range (less than 2×SE below age-matched reference).

threshold for scan positivity.[25] That is, a subject with a DVR value that is below this line (ie, a value that is more than two standard errors below age-matched reference) could possibly have an abnormal dopaminergic system.

Linear regression parameters and their 95% confidence intervals for each regional DVR are summarized in Table 6 for both databases.

Table 6. Linear regression analysis (R values, intercepts, and slopes) of DAT availability versus age and irrespective of gender. Values in parentheses are 95% confidence intervals for the intercepts and slopes.

Database	Regression parameters	Caudate	Putamen	Anterior Putamen	Posterior Putamen	Striatum
Flash3D	Intercept	5.004 (4.78, 5.23)	5.055 (4.84, 5.27)	5.134 (4.91, 5.36)	4.942 (4.73, 5.16)	5.028 (4.81, 5.24)
	Slope	-0.015 (-0.018, -0.011)	-0.018 (-0.021, -0.015)	-0.017 (-0.021, -0.013)	-0.019 (-0.023, -0.016)	-0.016 (-0.019, -0.013)
	2×SE	0.83	0.80	0.86	0.80	0.80
	R^2	0.22	0.32	0.27	0.36	0.27
FBP	Intercept	4.585 (4.40, 4.77)	4.434 (4.26, 4.61)	4.541 (4.35, 4.73)	4.289 (4.12, 4.46)	4.521 (4.34, 4.7)
	Slope	-0.015 (-0.018, -0.013)	-0.015 (-0.018, -0.013)	-0.015 (-0.018, -0.012)	-0.016 (-0.019, -0.013)	-0.015 (-0.018, -0.012)
	2×SE	0.68	0.67	0.71	0.64	0.66
	R^2	0.32	0.34	0.30	0.37	0.33

Asymmetries and Putamen-to-Caudate Ratios

There was no clear age effect on the asymmetry values or on the P/C ratios. For each of these parameters, comparisons of patients' values are each completed with respect to the sample mean (ie, mean of all corresponding reference values in the database). The sample means and SDs of the left and right P/C ratios and asymmetry values are summarized in Table 7 for both databases.

A new scan acquired and reconstructed using the same protocols as the reference values should raise the possibility of alteration of the presynaptic dopaminergic system when its left or right P/C ratio is two SDs below the reference mean, or when one of its asymmetries is two SDs above corresponding reference mean. For example, striatum asymmetry calculated from a ^{123}I-FP-CIT[a] image similarly processed as the Flash3D database, is considered normal when lower than 7.84%.

Table 7. Left and right putamen to caudate ratios and asymmetry values for Flash3D and FBP databases. Asymmetries are given as %. Values are given as mean±SD. P/C: putamen to caudate ratio.

	Left P/C ratio	Right P/C ratio	Striatum Asymmetry	Caudate Asymmetry	Putamen Asymmetry
Flash 3D	0.96±0.05	0.96±0.05	3.02±2.41	3.56±2.62	3.68±2.53
FBP	0.95±0.04	0.96±0.04	2.44±1.91	3.09±2.33	2.73±2.17

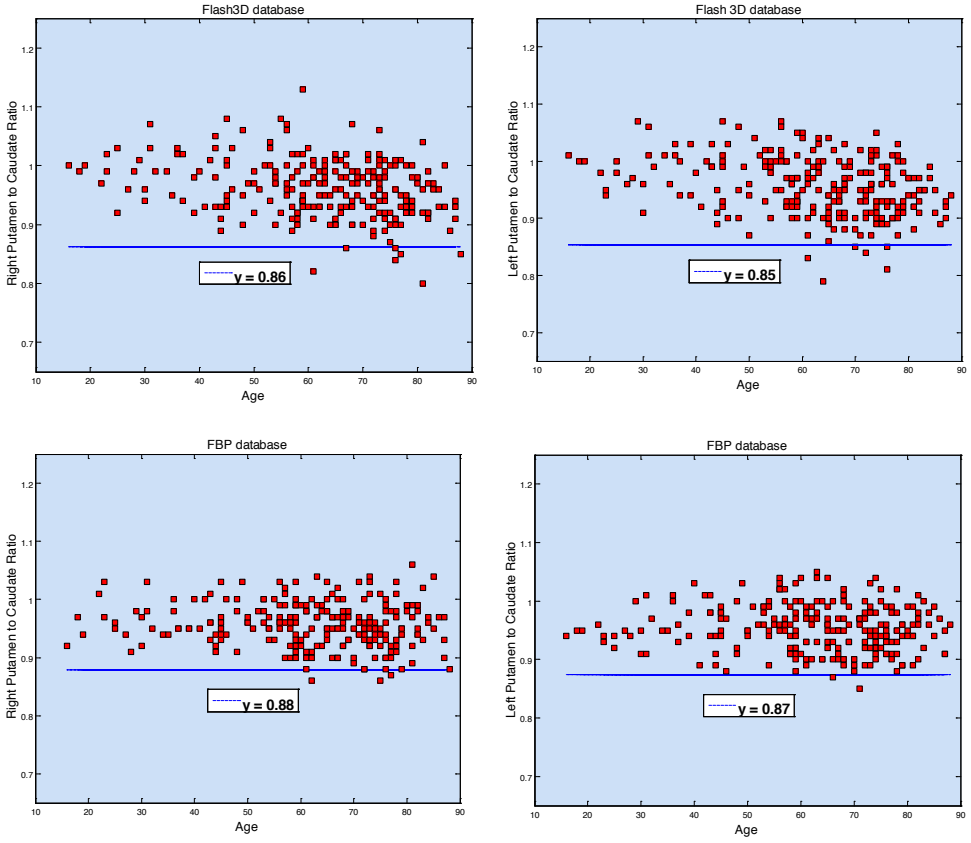

Figure 11. Left and right P/C ratios for Flash3D (above) and FBP (bottom row) databases. A general reference value, y, is given as mean-2×standard deviations of corresponding values in the database; y defines the line below which a scan could be suspected as being positive.

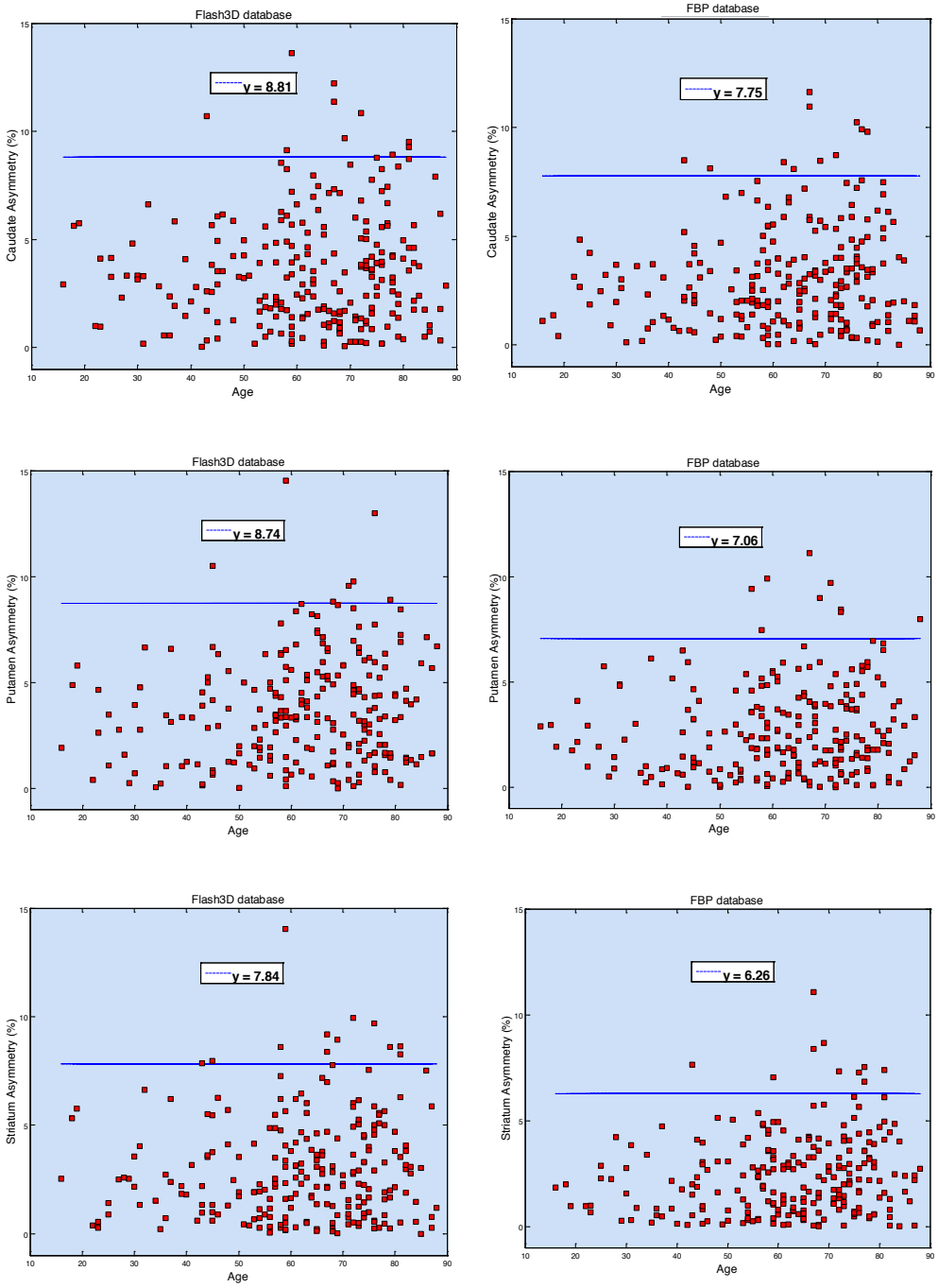

Figure 12. Asymmetry values (%) corresponding to caudate, putamen, and striatum (from top to bottom) and for Flash3D (left) and FBP (right) databases. The solid blue line (y = mean + 2 × standard deviations of corresponding reference values) defines the reference limit above which a scan could be suspected as being positive.

Comparison to reconstructed ^{123}I-FP-CIT[a] databases

For a test subject of a given age, each of its regional DVR values is calculated and displayed along with its corresponding predicted and age-matched reference DVR value. The latter is calculated by substituting the subject's age in the equation of the appropriate regression line. Using the line equation of the lower bounding line of the predictive interval (y=slope×age+intercept-2×SE), the patient's age-matched normalcy threshold can also be calculated. For example, the DVR values of a healthy 70-year-old subject, calculated from a ^{123}I-FP-CIT[a] image processed as the data in the Flash3D database, are expected to be above -0.016x70+4.23=3.11 for the striatum, -0.018x70+4.26=3.0 for the putamen, and -0.015x70+4.17=3.12 for caudate, on both hemispheres.

The z-score for each of the measured DVR values is also estimated and displayed by taking the ratio of the difference between the measured and predicted age-matched DVRs over the SE of the regression model (eg, results' table in Figures 14 and 16). The z-scores give an estimate of the number of SEs that the patient's quantified DVR values are from their respective age-matched normal references.

Example 1

Figure 13 shows the slab view of a 61-year-old male patient with markedly reduced ^{123}I-FP-CIT[a] uptake on both left and right striata. This is a case that is easy to visually interpret as positive. The patient's data was compared to the Flash3D database. Left and right striatal DVR values are more than two SEs below the age-matched reference value as shown on the graphical display at the bottom left panel of Figure 14. Note that the user can select to graphically display other DVR values. The results table at the bottom right panel of Figure 14 summarize all quantified results. These results indicate that all quantified parameters fall within abnormal ranges.

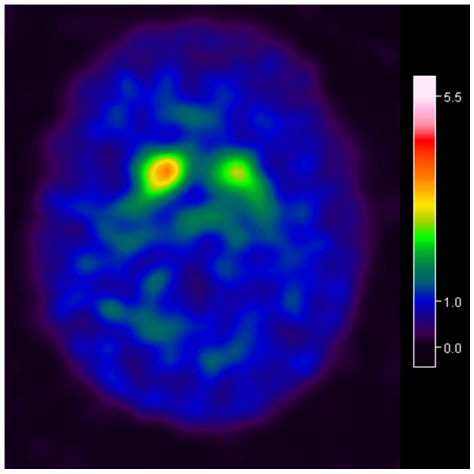

Figure 13. Slab view (averaged uptake ratios with respect to mean uptake within whole brain minus striatum VOI) corresponding to a 61-year-old male patient showing clear reduction of ^{123}I-FP-CIT[a] uptake on both left and right striatal regions.

Data courtesy of Hospices Civils de Lyon, Lyon, France.

Figure 14. Comparison results corresponding to the 61-year-old male patient shown in Figure 13. Top row: three-plane view (axial, coronal, and sagittal) of the fused patient's ^{123}I-FP-CIT[a] and CT images in the MNI space with overlays of the striatal (white) and the reference (green) volumes of interest. Bottom left: graphical display of the patient's left and right striatum DVR values (red and blue dots) compared to the corresponding reference values (grey dots). User can select to graphically display other DVR values. Bottom right: table displaying all quantitative results. Z-scores indicate that all quantified parameters fall within abnormal ranges. Results correspond to comparison with Flash3D database.

Data courtesy of Hospices Civils de Lyon, Lyon, France.

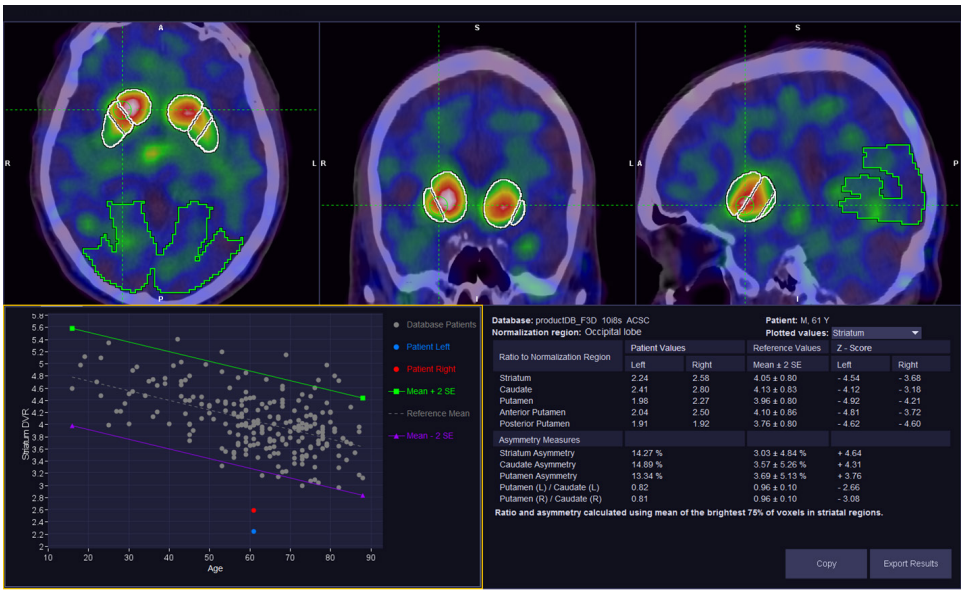

Example 2

The case shown in Figure 15 coresponds to a 63-year-old male patient whose ^{123}I-FP-CIT[a] uptake is uniformaly reduced on the left side. Qualitatively, one can clearly notice the uptake asymmetry with a clear reduction on the left side compared to the right side. However, without quantitative measures, it is not clear from the slab view alone if this is a positive or a negative case. This patient has major hydrocephalus which rendered the automatic positioning of the striatal VOIs to be challenging. Manual adjustments were carefully performed in order to accurately position the striatal and the occipital VOIs on the spatially normalized ^{123}I-FP-CIT[a] image. The corresponding quantified values (binding ratios and asymmetries) were all within normal ranges as shown on the results table in Figure 16. Results correspond to comparison with the FBP database.

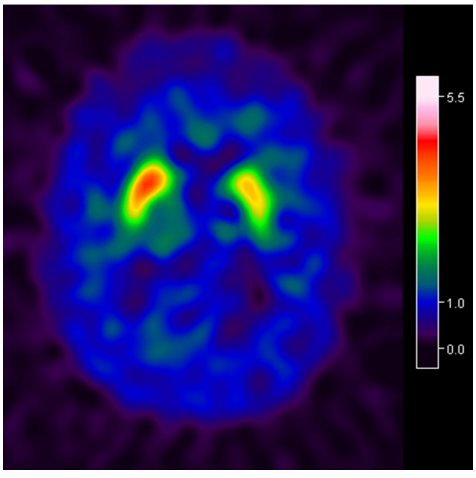

Figure 15. Slab view (averaged uptake ratios with respect to mean uptake within whole brain minus striatum VOI) corresponding to a 63-year-old male patient showing uniformly asymmetric uptake with a reduction on the left striatum.

Data courtesy of Hospices Civils de Lyon, Lyon, France.

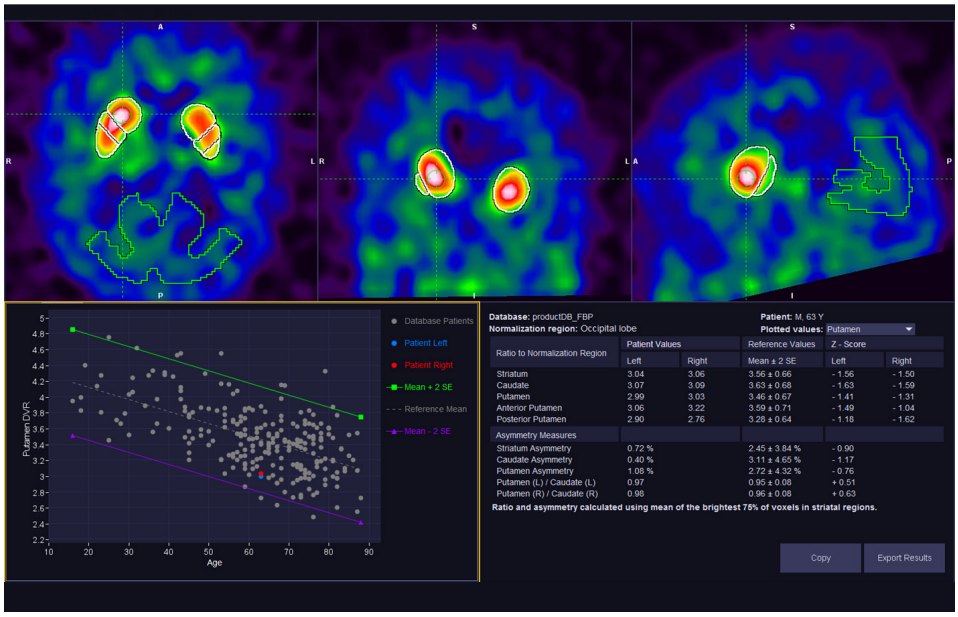

Figure 16. Comparison results corresponding to the 63-year-old male patient shown in Figure 15. Top row: three-plane view (axial, coronal, and sagittal) of the patient's image in the MNI space with overlays of the striatal (white) and the reference (green) volumes of interest. Bottom left: graphical display of the patient's left and right putamen DVR values (red and blue dots) compared to the corresponding reference DVR values (grey dots). User can select to graphically display other DVR values. Bottom right: table displaying all quantitative results. Z-scores indicate that all quantified parameters are within normal ranges. Results correspond to comparison with the FPB database.

Data courtesy of Hospices Civils de Lyon, Lyon, France.

Conclusion

Striatal Analysis of FDOPA[a] and ^{123}I-FP-CIT[a] images within *syngo*.via MI Neurology provides a tool for accurate visual interpretation of striatal uptake. In addition, Striatal Analysis is also a software system that supports VOI-based semi-quantitative analysis and comparison of a subject data to a database of normal reference values for a more objective evaluation of striatal uptake.

Users with access to "normal" data have the possibility of creating their own databases of reference values, for example, tailored for specific populations or for new tracers. Comparisons to such databases may be of greater help, in particular, for cases that are challenging to interpret visually. For example, challenges can be presented with very early degenerative conditions with borderline scans or (in case of ^{123}I-FP-CIT[a] SPECT) in clinically diseased patients with Scans without Evidence of Dopaminergic Deficit (or SWEDD). Age correction for tracers that are age-dependent (eg, ^{123}I-FP-CIT[a]) is performed when building a corresponding normal database to allow comparison of new subjects to age-matched reference values.

There are some important aspects that should be carefully considered when performing comparisons to a database of reference values. As quantitative measurements depend upon the imaging system as well as the reconstruction, correction and quantification methods, new scans should be acquired, reconstructed, and processed following the same protocols as the scans in the selected database. If a new scan is generated with different protocols than the ones used to compute the normative values, then some sort of calibration should be performed to harmonize measurements prior to conducting any comparisons.

Users should also be aware of imaging and processing artifacts for an accurate interpretation of the comparison results.

About the authors

Rachid Fahmi, PhD., received a M.Sc. and a Doctorate degree in Applied Mathematics from University of Metz, France and then completed a Ph.D. in Electrical and Computer Engineering at the University of Louisville, KY in 2008. He has worked in medical imaging since 2003 at the University of Louisville and at Case Western Reserve University, OH. He's been with the Research and Clinical Collaborations team of Siemens Molecular Imaging as staff scientist since the summer of 2015, leading scientific development of software solutions for molecular imaging applications in Neurology.

Günther Platsch, MD, studied medicine at the University of Erlangen-Nuremberg since 1982 and passed the final exams in 1988. From 1988 to 2004, he worked as an assistant physician, later as a senior physician at the department of Nuclear Medicine of that University. He received a Doctorate degree in Medicine in 1991 (Dr. med.) and became a board-certified Nuclear Medicine Physician in 1992. In 2004 Günther Platsch joined Siemens AG as a clinical scientist in Siemens Molecular Imaging, since 2011 as a Senior Key Expert. In this position he provides medical input for clinical application development as well as in SPECT and PET development.

References

[1] **Hughes AJ, Daniel SE, Kilford L, Lees AJ.** Accuracy of clinical diagnosis of idiopathic Parkinson's disease: a clinico-pathological study of 100 cases. *Journal of Neurology, Neurosurgery & Psychiatry.* 1992 Mar 1; 55(3):181-4.

[2] **Djang DS, Janssen MJ, Bohnen N, Booij J, Henderson TA, Herholz K, Minoshima S, Rowe CC, Sabri O, Seibyl J, Van Berckel BN.** SNM practice guideline for dopamine transporter imaging with ^{123}I-ioflupane SPECT 1.0. *Journal of Nuclear Medicine.* 2012; 53(1):154-63.

[3] **Booth TC, Nathan M, Waldman AD, Quigley AM, Schapira AH, Buscombe J.** The role of functional dopamine-transporter SPECT imaging in parkinsonian syndromes, part 1. *American Journal of Neuroradiology.* 2015 Feb 1; 36(2):229-35.

[4] **Booij J, Tissingh G, Winogrodzka A, van Royen EA.** Imaging of the dopaminergic neurotransmission system using single-photon emission tomography and positron emission tomography in patients with parkinsonism. European journal of nuclear medicine. 1999 Feb 1; 26(2):171-82.

[5] **Booij J, Speelman JD, Horstink MW, Wolters EC.** The clinical benefit of imaging striatal dopamine transporters with [^{123}I] FP-CIT SPET in differentiating patients with presynaptic parkinsonism from those with other forms of Parkinsonism. *European Journal of Nuclear Medicine.* 2001 Mar 1; 28(3):266-72.

[6] **Booij J, Tissingh G, Boer GJ, Speelman JD, Stoof JC, Janssen AG, Wolters EC, Van Royen EA.** [^{123}I] FP-CIT SPECT shows a pronounced decline of striatal dopamine transporter labelling in early and advanced Parkinson's disease. *Journal of Neurology, Neurosurgery & Psychiatry.* 1997 Feb 1; 62(2):133-40.

[7] **Walker Z, Costa DC, Walker RW, Shaw K, Gacinovic S, Stevens T, Livingston G, Ince P, McKeith IG, Katona CL.** Differentiation of dementia with Lewy bodies from Alzheimer's disease using a dopaminergic presynaptic ligand. *Journal of Neurology, Neurosurgery & Psychiatry.* 2002 Aug 1; 73(2):134-40.

[8] **Khan NL, Valente EM, Bentivoglio AR, Wood NW, Albanese A, Brooks DJ, Piccini P.** Clinical and subclinical dopaminergic dysfunction in PARK6-linked Parkinsonism: an ^{18}F-dopa PET study. *Annals of Neurology.* 2002 Dec 1; 52(6):849-53.

[9] **Darcourt J, Booij J, Tatsch K, Varrone A, Vander Borght T, Kapucu ÖL, Någren K, Nobili F, Walker Z, Van Laere K.** EANM procedure guidelines for brain neurotransmission SPECT using ^{123}I-labelled dopamine transporter ligands, version 2. *European Journal of Nuclear Medicine and Molecular Imaging.* 2010 Feb 1; 37(2):443-50.

[10] **Tondeur MC, Hambye AS, Dethy S, Ham HR.** Interobserver reproducibility of the interpretation of I-123 FP-CIT single-photon emission computed tomography. *Nuclear Medicine Communications.* 2010 Aug 1;31(8):717-25.

[11] **Booij J, Habraken JB, Bergmans P, Tissingh G.** Imaging of dopamine transporters with iodine-123-FP-CIT SPECT in healthy controls and patients with Parkinson's disease. *The Journal of Nuclear Medicine.* 1998 Nov 1; 39(11):1879.

[12] **Söderlund TA, Dickson JC, Prvulovich E, Ben-Haim S, Kemp P, Booij J, Nobili F, Thomsen G, Sabri O, Koulibaly PM, Akdemir OU.** Value of semiquantitative analysis for clinical reporting of ^{123}I-2-β-carbomethoxy-3β-(4-iodophenyl)-N-(3-fluoropropyl) nortropane SPECT studies. *Journal of Nuclear Medicine.* 2013 May 1; 54(5):714-22.

[13] **Tatsch K, Poepperl G.** Quantitative approaches to dopaminergic brain imaging. The quarterly journal of nuclear medicine and molecular imaging: official publication of the Italian Association of Nuclear Medicine (AIMN)[and] the *International Association of Radiopharmacology (IAR),*[and] *Section of the Society of...* 2012 Feb; 56(1):27-38.

[14] **Zubal IG, Early M, Yuan O, Jennings D, Marek K, Seibyl JP.** Optimized, automated striatal uptake analysis applied to SPECT brain scans of Parkinson's disease patients. *Journal of Nuclear Medicine.* 2007 Jun 1; 48(6):857-64.

[15] **Morton RJ, Guy MJ, Clauss R, Hinton PJ, Marshall CA, Clarke EA.** Comparison of different methods of DaTscan quantification. *Nuclear Medicine Communications.* 2005 Dec 1; 26(12):1139-46.

[16] **Towey DJ, Bain PG, Nijran KS.** Automatic classification of ^{123}I-FP-CIT (DaTscan) SPECT images. *Nuclear Medicine Communications.* 2011 Aug 1; 32(8):699-707.

[17] **Staff RT, Ahearn TS, Wilson K, Counsell CE, Taylor K, Caslake R, Davidson JE, Gemmell HG, Murray AD.** Shape analysis of ^{123}I-N-ω-fluoropropyl-2-β-carbomethoxy-3β-(4-iodophenyl) nortropane single-photon emission computed tomography images in the assessment of patients with parkinsonian syndromes. *Nuclear Medicine Communications.* 2009 Mar 1; 30(3):194-201.

[18] **Choi H, Ha S, Im HJ, Paek SH, Lee DS.** Refining diagnosis of Parkinson's disease with deep learning-based interpretation of dopamine transporter imaging. *NeuroImage: Clinical.* 2017 Jan 1; 16:586-94.

[19] **Buchert R, Hutton C, Lange C, Hoppe P, Makowski M, Bamousa T, Platsch G, Brenner W, Declerck J.** Semiquantitative slab view display for visual evaluation of ^{123}I-FP-CIT SPECT. *Nuclear Medicine Communications.* 2016 May 1; 37(5):509-18.

[20] **Buchert R, Berding G, Wilke F, Martin B, von Borczyskowski D, Mester J, Brenner W, Clausen M.** IBZM tool: a fully automated expert system for the evaluation of IBZM SPECT studies. *European Journal of Nuclear Medicine and Molecular Imaging.* 2006 Sep 1; 33(9):1073-83.

[21] **Tzourio-Mazoyer N, Landeau B, Papathanassiou D, Crivello F, Etard O, Delcroix N, Mazoyer B, Joliot M.** Automated anatomical labeling of activations in SPM using a macroscopic anatomical parcellation of the MNI MRI single-subject brain. *Neuroimage.* 2002 Jan 1; 15(1):273-89.

[22] **Abedelahi A, Hasanzadeh H, Hadizadeh H, Joghataie MT.** Morphometric and volumetric study of caudate and putamen nuclei in normal individuals by MRI: effect of normal aging, gender and hemispheric differences. *Polish Journal of Radiology.* 2013 Jul; 78(3):7-14.

[23] **Tatsch K, Poepperl G.** Nigrostriatal dopamine terminal imaging with dopamine transporter SPECT: an update. *Journal of Nuclear Medicine.* 2013 Aug 1;54(8):1331-8

[24] **Varrone A, Dickson JC, Tossici-Bolt L, Sera T, Asenbaum S, Booij J, Kapucu OL, Kluge A, Knudsen GM, Koulibaly PM, Nobili F.** European multicentre database of healthy controls for [^{123}I] FP-CIT SPECT (ENC-DAT): age-related effects, gender differences and evaluation of different methods of analysis. *European Journal of Nuclear Medicine and Molecular Imaging.* 2013 Jan 1; 40(2):213-27.

[25] **Nicastro N, Garibotto V, Poncet A, Badoud S, Burkhard PR.** Establishing on-site reference values for 123 I-FP-CIT SPECT (DaTscan®) using a cohort of individuals with non-degenerative conditions. *Molecular Imaging and Biology.* 2016 Apr 1; 18(2):302-12.

[26] **Nurmi E, Ruottinen HM, Bergman J, Haaparanta M, Solin O, Sonninen P, Rinne JO.** Rate of progression in Parkinson's disease: a 6-[^{18}F] fluoro-L-dopa PET study. *Movement disorders: official journal of the Movement Disorder Society.* 2001 Jul; 16(4):608-15.

[27] **Karrer TM, Josef AK, Mata R, Morris ED, Samanez-Larkin GR.** Reduced dopamine receptors and transporters but not synthesis capacity in normal aging adults: a meta-analysis. *Neurobiology of aging.* 2017 Sep 1; 57:36-46.

[28] **Pirker W, Asenbaum S, Hauk M, Kandlhofer S.** Imaging serotonin and dopamine transporters with ^{123}I-beta-CIT SPECT: Binding kinetics and effects of normal aging. *The Journal of Nuclear Medicine.* 2000 Jan 1; 41(1):36-44.

[29] **Hoffman JM, Melega WP, Hawk TC, Grafton SC, Luxen A, Mahoney DK, Barrio JR, Huang SC, Mazziotta JC, Phelps ME.** The effects of carbidopa administration on 6-[^{18}F] fluoro-L-dopa kinetics in positron emission tomography. *Journal of Nuclear Medicine.* 1992 Aug 1; 33(8):1472-7.

[30] **Fahmi, R., Platsch, G., Sadr, A.B., Gouttard, S., Thobois, S., Zuehlsdorff, S. and Scheiber, C.** Single-site ^{123}I-FP-CIT reference values from individuals with non-degenerative parkinsonism—comparison with values from healthy volunteers. *European Journal of Hybrid Imaging*. 2020 Mar 13; 4(1):1-25.

[31] **van Dyck CH, Seibyl JP, Malison RT, Laruelle M, Zoghbi SS, Baldwin RM, Innis RB.** Age-related decline in dopamine transporters: analysis of striatal subregions, nonlinear effects, and hemispheric asymmetries. *The American journal of geriatric psychiatry.* 2002 Jan 1; 10(1):36-43.

[32] **Eusebio A, Azulay JP, Ceccaldi M, Girard N, Mundler O, Guedj E.** Voxel-based analysis of whole-brain effects of age and gender on dopamine transporter SPECT imaging in healthy subjects. *European Journal of Nuclear Medicine and Molecular Imaging.* 2012 Nov 1; 39(11):1778-1783.

[33] **Ryding E, Lindström M, Brådvik B, Grabowski M, Bosson P, Träskman-Bendz L, Rosén I.** A new model for separation between brain dopamine and serotonin transporters in ^{123}I-β-CIT SPECT measurements: normal values and sex and age dependence. *European Journal of Nuclear Medicine and Molecular Imaging.* 2004 Aug 1; 31(8):1114-1118.

Please contact your local Siemens sales representative for the most current information or contact one of the addresses listed below. Note: Original images always lose a certain amount of detail when reproduced.

"Siemens Healthineers" is considered a brand name. Its use is not intended to represent the legal entity to which this product is registered. Please contact your local Siemens organization for further details.

All photographs © 2020 Siemens Healthcare GmbH. All rights reserved.

[a] Features may not be available in all countries. Availability is based on tracer clearance as well as software feature clearance. Future availability cannot be guaranteed.

Siemens Healthineers Headquarters
Siemens Healthcare GmbH
Henkestr. 127
91052 Erlangen, Germany
Phone: +49 9131 84-0
siemens-healthineers.com

Published by
Siemens Medical Solutions USA, Inc.
Molecular Imaging
2501 North Barrington Road
Hoffman Estates, IL 60192
USA
Phone: +1 847 304-7700
siemens-healthineers.com/mi